



Article

Hermite Wavelet Method for Nonlinear Fractional Differential Equations

Arzu Turan Dincel ^{1,*} , Sadiye Nergis Tural Polat ² and Pelin Sahin ¹

¹ Department of Mathematical Engineering, Yildiz Technical University, Davutpasa Campus, Esenler, Istanbul 34220, Turkey

² Department of Electronics and Communications Engineering, Yildiz Technical University, Davutpasa Campus, Esenler, Istanbul 34220, Turkey; nergis@yildiz.edu.tr

* Correspondence: artur@yildiz.edu.tr

Abstract: Nonlinear fractional differential equations (FDEs) constitute the basis for many dynamical systems in various areas of engineering and applied science. Obtaining the numerical solutions to those nonlinear FDEs has quickly gained importance for the purposes of accurate modelling and fast prototyping among many others in recent years. In this study, we use Hermite wavelets to solve nonlinear FDEs. To this end, utilizing Hermite wavelets and block-pulse functions (BPF) for function approximation, we first derive the operational matrices for the fractional integration. The novel contribution provided by this method involves combining the orthogonal Hermite wavelets with their corresponding operational matrices of integrations to obtain sparser conversion matrices. Sparser conversion matrices require less computational load, and also converge rapidly. Using the generated approximate matrices, the original nonlinear FDE is converted into an algebraic equation in vector-matrix form. The obtained algebraic equation is then solved using the collocation points. The proposed method is used to find a number of nonlinear FDE solutions. Numerical results for several resolutions and comparisons are provided to demonstrate the value of the method. The convergence analysis is also provided for the proposed method.

Keywords: numerical approximation for FDEs; Hermite wavelets; operational matrix for fractional derivatives



Citation: Turan Dincel, A.; Tural Polat, S.N.; Sahin, P. Hermite Wavelet Method for Nonlinear Fractional Differential Equations. *Fractal Fract.* **2023**, *7*, 346. <https://doi.org/10.3390/fractalfract7050346>

Academic Editors: Ivanka Stamova, Carla M.A. Pinto and Dana Copot

Received: 13 February 2023

Revised: 19 April 2023

Accepted: 20 April 2023

Published: 23 April 2023



Copyright: © 2023 by the authors. Licensee MDPI, Basel, Switzerland. This article is an open access article distributed under the terms and conditions of the Creative Commons Attribution (CC BY) license (<https://creativecommons.org/licenses/by/4.0/>).

1. Introduction

The real-valued orders of derivatives and integrals are used in fractional differential equations (FDEs). These real-valued orders of derivatives and integrals enable FDEs to model physical and applied scientific phenomena more precisely. However, it is exceedingly challenging to develop analytical solutions to many types of FDEs due to the extra complexity caused by arbitrary orders of derivation and integration. Therefore, finding precise and effective numerical solution techniques for the FDEs is essential. In recent years, certain numerical methods have been used for FDEs, such as the finite difference method [1], B-spline collocation method [2], differential transform method [3] Adomian decomposition method [4,5], variational iteration method [6,7], block-by-block method [8], orthogonal polynomials method [9–11], Galerkin method [12], Bessel collocation method [13], spectral method [14], reproducing kernel method [15,16], and operational matrix methods [17–19]. Similar to this, several wavelet types are currently being researched for issues including increased computational cost. Wavelets are mathematical operations that separate data into various time–frequency components. These functions are created by dilating and shifting a wavelet function known as the mother wavelet function. The fundamental benefit of the wavelet basis is that it simplifies the solution of the FDE problem to a set of algebraic equations. Additionally, the method converges quickly and easily due to the wavelets' many advantages, including their orthogonality, singularity detection skills, compact support, and simultaneous representation of data in several resolutions. Many wavelet basis

functions have been used to solve a wide range of FDEs. Legendre, Haar, Bernoulli, Euler, CAS, Taylor, Laguree, Chebyshev wavelets of first and second kind are employed in recent studies elsewhere [20–28].

In this paper we aim to solve nonlinear FDEs using Hermite wavelets. To the best of our knowledge, Hermite wavelets have not been exploited often. Furthermore, it is obvious that the orthogonal basis functions will provide sparser operational matrices used for the numerical approximations of the fractional differential terms. In this paper, we first obtain the operational matrices for fractional integration using Hermite wavelets and block-pulse functions (BPF) for function approximation. The operational matrices for the fractional integration obtained using BPF is not the same as the ones obtained in [29]. Our approximation produces fewer calculations and an easier conversion from the nonlinear FDEs in question into the system of algebraic equations. The novelty of the method lies in the fact that the method combines the orthogonal Hermite wavelets with their corresponding operational matrices of integration to obtain sparser conversion matrices, which smoothly convert the FDE to a corresponding algebraic equation in vector-matrix form. Calculating the algebraic equation for a few collocation points creates a system of algebraic equations. By solving for the coefficients, the approximate solution is also obtained. The proposed method consists of simple and clear steps, therefore it is straightforward to code in any programming language of choice.

The paper is organized as follows: In Section 2, the fundamental definitions of fractional calculus are given. In Section 3, The Hermite wavelets are defined. The operational matrices for nonlinear FDEs are obtained using Hermite wavelets in Section 4. Convergence analysis is presented in Section 5. The proposed method is presented in Section 6. Numerical solutions for several nonlinear FDEs are provided in Section 7. The paper is concluded in Section 8.

2. Foundations

The preliminary definitions for fractional calculus that are utilized in the paper are presented in this section.

Definition 1. *Of the many possible definitions for fractional derivatives, Riemann–Liouville and Caputo are the most commonly used [30]. The Riemann–Liouville fractional integral operator of order $\alpha \geq 0$ is defined by [30]:*

$$(I^\alpha f)(t) = \begin{cases} \frac{1}{\Gamma(\alpha)} \int_0^t \frac{f(\tau)}{(t-\tau)^{1-\alpha}} d\tau & \alpha > 0, t > 0 \\ 0 & \alpha = 0 \end{cases} \quad (1)$$

Riemann–Liouville derivatives possess some disadvantages for modeling real world phenomena with FDEs. Therefore, a modified fractional differential operator $D^\alpha f$ is more commonly used, which is proposed by Caputo [30].

Definition 2. *The Caputo definition of the fractional derivative operator is given by [30]:*

$$(D^\alpha f)(t) = \begin{cases} \frac{d^n f(t)}{dt^n} & \alpha = n \in \mathbb{R} \\ \frac{1}{\Gamma(n-\alpha)} \int_0^t \frac{f^{(n)}(\tau)}{(t-\tau)^{1-n+\alpha}} d\tau & 0 \leq n-1 < \alpha < n \end{cases} \quad (2)$$

The following expressions relate the Riemann–Liouville operator and Caputo operator:

$$(D^\alpha I^\alpha f)(t) = f(t) \quad (3)$$

and

$$(I^\alpha D^\alpha f)(t) = f(t) - \sum_{k=0}^{n-1} f^{(k)}(0^+) \frac{t^k}{k!} \tag{4}$$

3. Hermite Wavelets (HWs)

Wavelets are defined as a group of wavelike functions. They are formulated by dilating and translating a so called mother wavelet function $\Psi(t)$. The family of continuous wavelets can be obtained using translation parameter b and the dilation parameter a , as follows [29]:

$$\Psi_{a,b}(t) = |a|^{-1/2} \Psi\left(\frac{t-b}{a}\right), \quad a, b \in \mathbb{R}, a \neq 0. \tag{5}$$

When we restrict a and b to only have discrete values, we can derive the matching family of discrete wavelets such that $a = a_0^{-k}, b = nb_0 a_0^{-k}$ where $a_0 > 1, b_0 > 0$, which results in:

$$\Psi_{kn}(t) = |a_0|^{k/2} \Psi(a_0^k t - nb_0), \quad k, n \in \mathbb{Z}. \tag{6}$$

We can define Hermite wavelets on the time interval $[0, 1]$ in [29] as:

$$\Psi_{nm}(t) = \begin{cases} \frac{2^{(k+1)/2}}{\sqrt{\pi}} H_m(2^k t - 2n + 1), & \frac{n-1}{2^{k-1}} \leq t \leq \frac{n}{2^{k-1}} \\ 0, & \text{otherwise} \end{cases} \tag{7}$$

where $n = 0, 1, \dots, 2^k - 1, m = 0, 1, \dots, M - 1$, and these $H_m(t)$ polynomials, with respect to the weight function $\omega(t) = e^{-t^2}$, are Hermite polynomials of degree m . The Hermite polynomials can be defined using the recurrence formula:

$$H_{m+2}(t) = 2tH_{m+1}(t) - 2(m+1)H_m(t), \quad m = 0, 1, 2, \dots \tag{8}$$

where $H_0(t) = 1, H_1(t) = 2t$. The polynomials have the following property, which is used in the convergence analysis below:

$$H'_{m+1}(t) = 2(m+1)H_m(t). \tag{9}$$

4. Function Approximation of HWs

If a function $y(t)$ is squarely integrable in $[0, 1]$, we can approximate $y(t)$ using Hermite wavelets as:

$$y(t) = \sum_{n=0}^{\infty} \sum_{m \in \mathbb{Z}} c_{nm} \Psi_{nm}(t) = C^T \Psi(t), \tag{10}$$

where $c_{nm} = \langle y(t), \Psi_{nm}(t) \rangle_{L^2_{\omega}[0,1]} = \int_0^1 y(t) \Psi_{nm}(t) \omega_n(t) dt$, in which $\langle \cdot, \cdot \rangle_{L^2_{\omega}[0,1]}$ denotes the inner product in $L^2_{\omega}[0, 1]$ and $y(t)$ can be estimated by the finite series such as:

$$y(t) \approx \sum_{n=0}^{2^k-1} \sum_{m=0}^{M-1} c_{nm} \Psi_{nm}(t) = C^T \Psi(t), \tag{11}$$

where Hermite coefficient vector C and Hermite wavelet vector $\Psi(t)$ are given as:

$$C = \left[c_{10}, c_{11}, \dots, c_{1(M-1)}, c_{20}, c_{21}, \dots, c_{2(M-1)} \dots c_{2^{k-1}0}, c_{2^{k-1}1}, \dots, c_{2^{k-1}(M-1)} \right]^T, \tag{12}$$

$$\Psi = \left[\Psi_{10}, \Psi_{11}, \dots, \Psi_{1(M-1)}, \Psi_{20}, \Psi_{21}, \dots, \Psi_{2(M-1)} \dots \Psi_{2^{k-1}0}, \Psi_{2^{k-1}1}, \dots, \Psi_{2^{k-1}(M-1)} \right]^T \tag{13}$$

The Hermite wavelet matrix is defined as:

$$\phi_{m'xm'} = [\Psi(t_1), \Psi(t_2), \Psi(t_3), \dots, \Psi(t_{m'})], \tag{14}$$

where $m' = 2^{k-1}M$ and t_i are collocation points. If the collocation points are chosen as $t_i = \frac{i-0.5}{m'}$, $i = 1, 2, 3, \dots, m'$, the Hermite wavelet matrix for $k = 2$, $M = 3$, and $\alpha = 0.5$ becomes:

$$\phi_{m'xm'} = \begin{bmatrix} 1.5958 & 1.5958 & 1.5958 & 0 & 0 & 0 \\ -2.1277 & 0 & 2.1277 & 0 & 0 & 0 \\ -0.3546 & -3.1915 & -0.3546 & 0 & 0 & 0 \\ 0 & 0 & 0 & 1.5958 & 1.5958 & 1.5958 \\ 0 & 0 & 0 & -2.1277 & 0 & 2.1277 \\ 0 & 0 & 0 & -0.3546 & -3.1915 & -0.3546 \end{bmatrix},$$

where the $\Psi(t)$ vector can be given as $\Psi(t) = \frac{2^{3/2}}{\sqrt{\pi}} [1 \quad 8t - 2 \quad 64t^2 - 32t + 2 \quad 0 \quad 0 \quad 0]$ for the first three collocation points and $\Psi(t) = \frac{2^{3/2}}{\sqrt{\pi}} [0 \quad 0 \quad 0 \quad 1 \quad 8t - 6 \quad 64t^2 - 96t + 34]$ for the next three collocation points for $k = 2$, $M = 3$.

The following analysis looks at the uniform convergence requirements for the decomposition of $y(t)$.

5. Convergence Analysis

Theorem 1: *If y on $[0, 1]$ is a continuous function, then $|y(t)| < R$ can be represented by the sum of an infinite number of Hermite wavelets, then the series uniformly converge to $y(t)$.*

Proof

$$c_{nm} = \int_0^1 y(t) \Psi_{nm}(t) dt = \int_{(n-1)/2^{k-1}}^{n/2^{k-1}} y(t) \frac{2^{(k+1)/2}}{\sqrt{\pi}} H_m(2^k t - 2n + 1) dt. \tag{15}$$

Using the change of variables as $2^k t - 2n + 1 = x$ and $2^k dt = dx$, we obtain:

$$c_{nm} = \frac{2^{(1-k)/2}}{\sqrt{\pi}} \int_{-1}^1 y\left(\frac{x - 1 + 2n}{2^k}\right) H_m(x) dx. \tag{16}$$

Employing mean-value problem for integral calculus yields:

$$c_{nm} = \frac{2^{(1-k)/2}}{\sqrt{\pi}} y\left(\frac{z - 1 + 2n}{2^k}\right) \int_{-1}^1 H_m(x) dx \text{ for } z \in (-1, 1). \tag{17}$$

Using the derivative property of the Hermite polynomials given in Equation (9), we obtain:

$$c_{nm} = \frac{2^{(1-k)/2}}{\sqrt{\pi}} y\left(\frac{z - 1 + 2n}{2^k}\right) \int_{-1}^1 \frac{H'_{m+1}(x)}{2(m+1)} dx = \frac{2^{(1-k)/2}}{\sqrt{\pi}} y\left(\frac{z - 1 + 2n}{2^k}\right) \frac{H_{m+1}(x)}{2(m+1)} \Big|_{-1}^1. \tag{18}$$

Because $y(t)$ is bounded and $n \leq 2^{k-1}$, we can write:

$$|c_{nm}| \leq \frac{2^{(1-k)/2}}{\sqrt{\pi}} R \frac{|H_{m+1}(1) - H_{m+1}(-1)|}{2(m+1)} \leq \frac{1}{\sqrt{n\pi}} R \frac{|H_{m+1}(1) - H_{m+1}(-1)|}{2(m+1)}. \tag{19}$$

Therefore, $\sum_{n=1}^{\infty} \sum_{m=0}^{\infty} c_{nm}$ does absolutely converge. Hence, the HWs expansion of $y(t)$ given in (10) converges uniformly [29]. \square

6. Operational Matrices of HWs

In this section we obtain the fractional operational matrices of Hermite wavelets. Fractional operational matrices of HWs require less computation with Block Pulse Functions (BPFs). Consequently, it is simpler to convert the FDE into an algebraic vector-matrix-form equation. All the numerical calculations are performed using Matlab R2021b in this study.

An m' set of BPFs is defined as:

$$b_i(t) = \begin{cases} 1 & (i-1)/m' \leq t < i/m' \\ 0 & \text{otherwise} \end{cases}, \tag{20}$$

where $i = 1, 2, 3, \dots, m'$. The functions $b_i(t)$ are disjoint and orthogonal. For $t \in [0, 1)$,

$$b_i(t)b_j(t) = \begin{cases} 0 & i \neq j \\ b_i(t) & i = j \end{cases}, \tag{21}$$

$$\int_0^1 b_i(\tau)b_j(\tau) d\tau = \begin{cases} 0 & i \neq j \\ 1/m' & i = j \end{cases}, \tag{22}$$

Any squarely integrable function $f(t)$ defined in $[0, 1)$ can be expanded into an m' set of BPFs as:

$$f(t) = \sum_{i=1}^{m'} f_i b_i(t) = f^T B_{m'}(t) \tag{23}$$

where $f = [f_1, f_2, \dots, f_{m'}]^T$, $B_{m'}(t) = [b_1(t), b_2(t), \dots, b_{m'}(t)]^T$ and f_i are given as $f_i = \frac{1}{m'} \int_{(i-1)/m'}^{i/m'} f(t) b_i(t) dt$.

Definition : Let $F = [f_1, f_2, \dots, f_{m'}]^T$ and $G = [g_1, g_2, \dots, g_{m'}]^T$. By means of BPFs, we have:

$$F_{m'}^T * G_{m'}^T == f_1g_1 + f_2g_2 + \dots + f_{m'}g_{m'}, \tag{24}$$

$$F^n = [f_1^n, f_2^n, \dots, f_{m'}^n]^T. \tag{25}$$

The HW matrix can also be expanded to an m' set of BPFs as:

$$\Psi(t) = \phi_{m'xm'} B_{m'}(t). \tag{26}$$

The Block Pulse operational matrix for fractional integration F^α is defined as [31]:

$$(I^\alpha B_{m'})(t) \approx F^\alpha B_{m'}(t), \tag{27}$$

where

$$F^\alpha = \frac{1}{m^\alpha} \frac{1}{\Gamma(\alpha + 2)} \begin{bmatrix} 1 & \zeta_1 & \zeta_2 & \zeta_3 & \dots & \zeta_{m'-1} \\ 0 & 1 & \zeta_1 & \zeta_2 & \dots & \zeta_{m'-2} \\ 0 & 0 & 1 & \zeta_1 & \dots & \zeta_{m'-3} \\ \vdots & \vdots & \ddots & \ddots & \vdots & \vdots \\ 0 & 0 & \dots & 0 & 1 & \zeta_1 \\ 0 & 0 & \dots & 0 & 0 & 1 \end{bmatrix}, \tag{28}$$

with $\zeta_k = (k + 1)^{\alpha+1} - 2k^{\alpha+1} + (k - 1)^{\alpha+1}$.

The fractional integration of the Hermite wavelet vector $\Psi(t)$ defined in (13) can be approximated as:

$$(I^\alpha \Psi)(t) \approx P_{m' \times m'}^\alpha \Psi(t), \tag{29}$$

where matrix $P_{m' \times m'}^\alpha$ is called the Hermite wavelet operational matrix.

Using Equations (26)–(29), we obtain:

$$(I^\alpha \Psi)(t) \approx (I^\alpha \phi_{m'xm'} B_{m'})(t) = \phi_{m'xm'} (I^\alpha B_{m'})(t) \approx \phi_{m'xm'} F^\alpha B_{m'}(t), \tag{30}$$

$$P_{m'xm'}^\alpha \Psi(t) \approx (I^\alpha \Psi)(t) \approx \phi_{m'xm'} F^\alpha B_{m'}(t) = \phi_{m'xm'} F^\alpha \phi_{m'xm'}^{-1} \Psi(t).$$

The resulting Hermite wavelet operational matrix $P_{m'xm'}^\alpha$ becomes:

$$P_{m'xm'}^\alpha \approx \phi_{m'xm'} F^\alpha \phi_{m'xm'}^{-1} \tag{31}$$

As an example, the Hermite wavelet operational matrix for $k = 2, M = 3$, and $\alpha = 0.5$ yields

$$P_{m' \times m'}^\alpha = \begin{bmatrix} 0.5116 & 0.1575 & -0.0250 & 0.4582 & -0.0754 & 0.0215 \\ -0.0818 & 0.2243 & 0.1287 & 0.1050 & -0.0449 & 0.0192 \\ -0.2999 & -0.2046 & 0.1854 & -0.3533 & 0.0501 & -0.0115 \\ 0 & 0 & 0 & 0.5116 & 0.1575 & -0.0250 \\ 0 & 0 & 0 & -0.0818 & -0.0818 & 0.1287 \\ 0 & 0 & 0 & -0.2999 & -0.2046 & 0.1854 \end{bmatrix}.$$

7. Numeric Solution Examples

This section includes several nonlinear FDE examples to show the effectiveness and compactness of the suggested approach.

Example 1:

We first analyze the following FDE, which can be used to model a solid material in a Newtonian fluid [30], defined as:

$$\begin{aligned} D^2 y(t) + D^{0.5} y(t) + y(t) &= 8 \\ y(0) = 0, y'(0) &= 0. \end{aligned} \tag{32}$$

Applying the proposed method, we have:

$$D^2 y(t) \simeq C^T \Psi(t), \tag{33}$$

$$D^{0.5} y(t) \simeq C^T P_{m'xm'}^{1.5} \Psi(t), \tag{34}$$

$$y(t) \simeq C^T P_{m'xm'}^2 \Psi(t) + y(0) = C^T P_{m'xm'}^2 \Psi(t). \tag{35}$$

Using the approximations of (33)–(35) in (32), we obtain:

$$C^T \phi_{m'xm'} + C^T P_{m'xm'}^{1.5} \phi_{m'xm'} + C^T P_{m'xm'}^2 \phi_{m'xm'} = [8, 8, \dots 8]. \tag{36}$$

Equation (36) is written for a few collocation points to construct an algebraic system of equations. The solution of that system provides the values of the coefficient vector C , which in turn provides the approximate solution.

The absolute errors, calculated as absolute difference between the exact and approximate solutions, is presented for several m' parameters in Table 1. As can be seen from Table 1, the Hermite Wavelet Method (HWM) error decreases with the increased resolution. The absolute errors are approximately on the order of E-4, E-5 for $m' = 48$, on the order of E-5, E-6 for $m' = 96$, and on the order of E-6, E-7 for $m' = 192$. A comparison with the Orthogonal Function Method (OFM) [32], Variational Iteration Method (VIM) [4], Adomian

Decomposition Method (ADM) [4], and the Finite Difference Method (FDM) [1] is presented in Table 2. As can be seen from the table, the proposed method can be said to converge better than the other methods. The exact solution and HWM results for $t \in [0, 1)$ are plotted in Figure 1. As can be seen from the figure, the numerical solution follows the exact solution closely.

Table 1. The absolute errors for HWM for several m' of example 1.

t	$m' = 24$	$m' = 48$	$m' = 96$	$m' = 192$
0	5.27×10^{-4}	1.40×10^{-4}	3.58×10^{-5}	9.01×10^{-6}
0.1	5.23×10^{-4}	1.31×10^{-4}	3.32×10^{-5}	8.32×10^{-6}
0.2	4.15×10^{-4}	1.09×10^{-4}	2.71×10^{-5}	6.56×10^{-6}
0.3	3.29×10^{-4}	7.49×10^{-5}	1.88×10^{-5}	4.80×10^{-6}
0.4	1.77×10^{-4}	4.36×10^{-5}	9.96×10^{-6}	2.62×10^{-6}
0.5	1.94×10^{-4}	2.37×10^{-5}	3.11×10^{-6}	6.66×10^{-7}
0.6	1.74×10^{-4}	4.29×10^{-5}	9.86×10^{-6}	2.81×10^{-6}
0.7	3.41×10^{-4}	7.54×10^{-5}	1.90×10^{-5}	4.93×10^{-6}
0.8	4.26×10^{-4}	1.17×10^{-4}	2.91×10^{-5}	7.17×10^{-6}
0.9	5.68×10^{-4}	1.43×10^{-4}	3.70×10^{-5}	9.22×10^{-6}

Table 2. Comparison with Orthogonal Function Method (OFM) [32], Variational Iteration Method (VIM) [4], Adomian Decomposition Method (ADM) [4], and the Finite Difference Method (FDM) [1], and the exact result of example 1 for $\alpha = 1$.

t	y_{exact}	y_{HWM} ($k = 8, M = 3$)	y_{OFM} [32]	y_{VIM} [4]	y_{ADM} [4]	y_{FDM} [1]
0.1	0.039750	0.039752	0.039754	0.039874	0.039874	0.039473
0.2	0.157036	0.157038	0.157043	0.158512	0.158512	0.157703
0.3	0.347370	0.347371	0.347373	0.353625	0.353625	0.352402
0.4	0.604695	0.604696	0.604699	0.622083	0.622083	0.620435
0.5	0.921768	0.921768	0.921768	0.960047	0.960047	0.957963
0.6	1.290457	1.290456	1.290458	1.363093	1.363093	1.360551
0.7	1.702008	1.702007	1.702007	1.826257	1.826257	1.823267
0.8	2.147287	2.147285	2.147286	2.344224	2.344224	2.340749
0.9	2.617001	2.616999	2.616998	2.911278	2.911278	2.907324

Example 2:

Consider the Riccati FDE [33] given below for $0 < \alpha \leq 1$ and $0 \leq t < 1$:

$$D^\alpha y(t) - y^2(t) = 1 \text{ with } y(0) = 0. \quad (37)$$

The exact solution for $\alpha = 1$ is given as $y = \tan(t)$.

The application of HWM to the Riccati FDE requires the approximate expressions listed below:

$$D^\alpha y(t) \simeq C^T \Psi(t), \quad (38)$$

$$y(t) \simeq C^T P_{m'xm'}^\alpha \Psi(t) + y(0) = C^T P_{m'xm'}^\alpha \phi_{m'xm'} B_{m'}. \quad (39)$$

Defining $C^T P_{m'xm'}^\alpha \phi_{m'xm'} = [a_1, a_2, \dots, a_{m'}]$, we have:

$$[y(t)]^2 = [a_1^2, a_2^2, \dots, a_{m'}^2] B_{m'}(t). \tag{40}$$

Combining all approximations in the original Riccati FDE gives:

$$C^T \phi_{m'xm'} - [a_1^2, a_2^2, \dots, a_{m'}^2] = [1, 1, \dots, 1]. \tag{41}$$

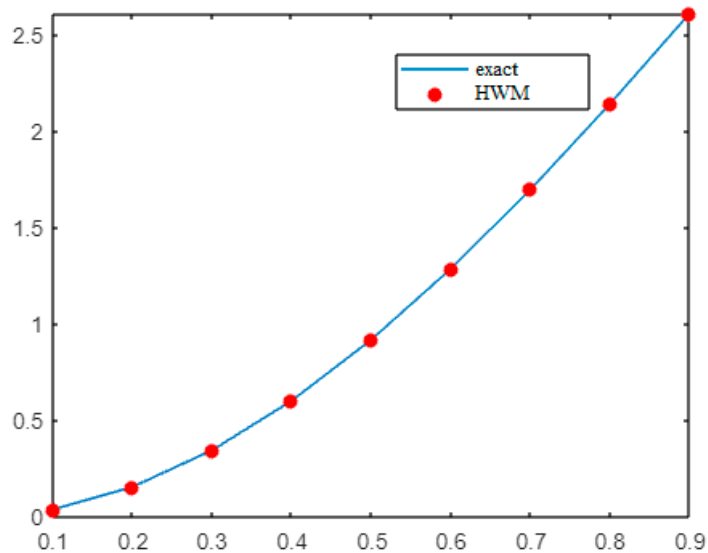


Figure 1. HWM result for $\alpha = 1$ with the exact solution of example 1 for $m' = 24$.

The solution for (41) is obtained as with the previous example through the algebraic system of equations which is constructed using a few collocation points.

Table 3 presents the method’s absolute errors for a number of m' parameters. The error diminishes with an increase in m' , as seen in Table 3. The absolute errors are approximately on the order of E-5 for $m' = 48$, on the order of E-5, E-6 for $m' = 96$, and on the order of E-6, E-7 for $m' = 192$. The HWM results and exact solution are given for $t \in [0, 1)$ in Figure 2. The FDE solutions for a few fractional values of α are presented in Figure 3. Figure 3 demonstrates that, as the fractional α approaches 1, the solution approximates to the exact solution obtained for integer order Riccati differential equation.

Table 3. The absolute errors for HWM for several m' of example 2.

t	$m' = 12$	$m' = 24$	$m' = 48$	$m' = 96$	$m' = 192$
0	3.79×10^{-4}	4.57×10^{-5}	5.67×10^{-6}	7.07×10^{-7}	8.83×10^{-8}
0.1	6.20×10^{-5}	3.38×10^{-5}	8.23×10^{-6}	1.78×10^{-6}	4.48×10^{-7}
0.2	2.87×10^{-4}	7.03×10^{-5}	1.51×10^{-5}	3.80×10^{-6}	9.89×10^{-7}
0.3	3.63×10^{-4}	9.45×10^{-5}	2.67×10^{-5}	6.64×10^{-6}	1.61×10^{-6}
0.4	7.33×10^{-4}	1.52×10^{-4}	3.84×10^{-5}	1.01×10^{-5}	2.52×10^{-6}
0.5	2.26×10^{-3}	3.72×10^{-4}	7.51×10^{-5}	1.68×10^{-5}	3.97×10^{-6}
0.6	1.25×10^{-3}	3.76×10^{-4}	9.34×10^{-5}	2.24×10^{-5}	5.61×10^{-6}
0.7	2.39×10^{-3}	5.92×10^{-4}	1.36×10^{-4}	3.43×10^{-5}	8.75×10^{-6}
0.8	3.17×10^{-3}	8.29×10^{-4}	2.26×10^{-4}	5.64×10^{-5}	1.38×10^{-5}
0.9	6.76×10^{-3}	1.41×10^{-3}	3.58×10^{-4}	9.36×10^{-5}	2.34×10^{-5}

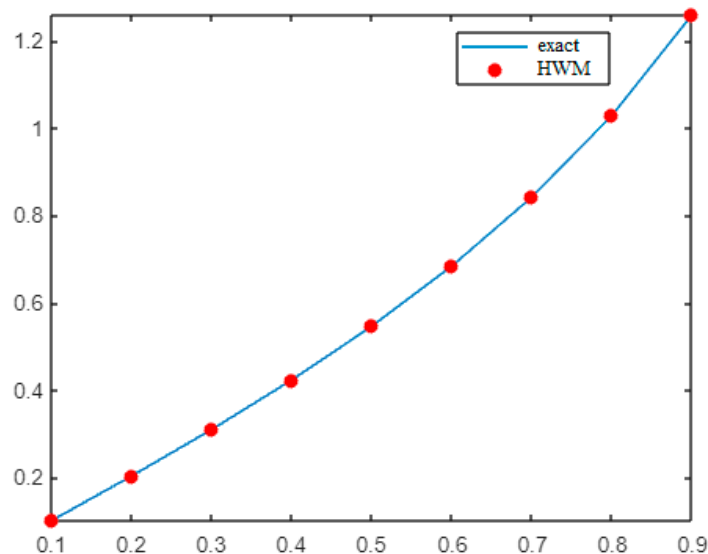


Figure 2. HWM result for $\alpha = 1$ with the exact solution of example 2 for $m' = 12$.

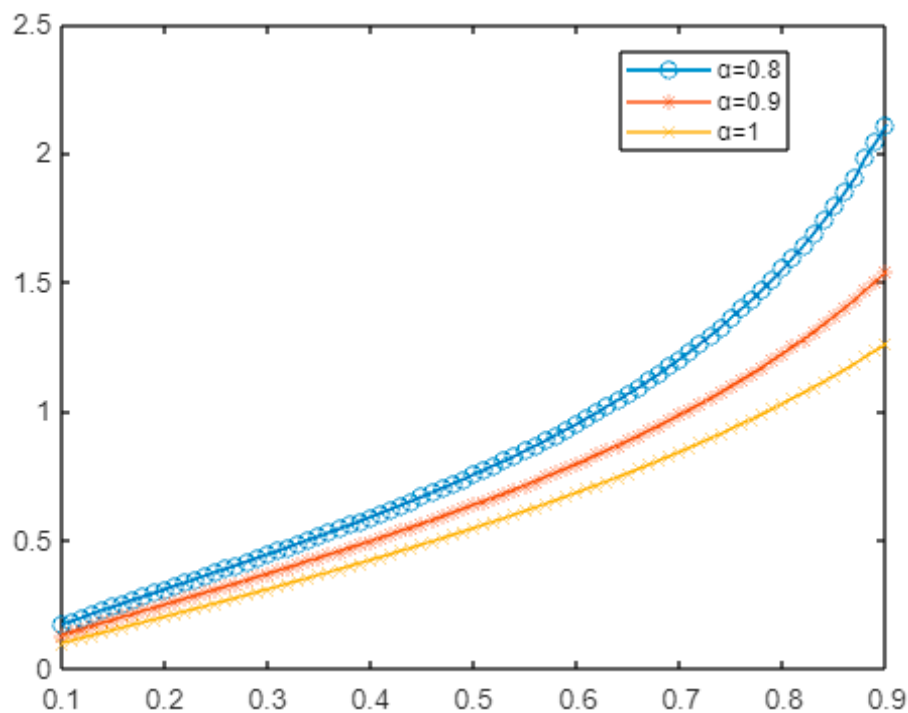


Figure 3. HWM result for several values of α of example 2 for $m' = 12$.

Example 3:

Consider the FDE [30] given again for $0 < \alpha \leq 1$ and $0 \leq t < 1$:

$$D^\alpha y(t) - (1 - y(t))^4 = 0 \text{ with } y(0) = 0. \tag{42}$$

The exact solution for $\alpha = 1$ is given as $y(t) = 1 - (1 + 3t)^{-1/3}$.

The application of HWM to the FDE results in:

$$C^T \phi_{m'xm'} - ([1, 1, \dots, 1] + 4[a_1, a_2, \dots, a_{m'}] + 6[a_1^2, a_2^2, \dots, a_{m'}^2] - 4[a_1^3, a_2^3, \dots, a_{m'}^3] + [a_1^4, a_2^4, \dots, a_{m'}^4]) = 0 \tag{43}$$

where $C^T P_{m'xm'}^\alpha \phi_{m'xm'} = [a_1, a_2, \dots, a_{m'}]$.

The solution of (43) is obtained as in the previous examples. Table 4 includes absolute errors for several m' . As expected, larger m' values provide lower error values. The absolute errors are approximately on the order of E-5, E-6 for $m' = 48$, on the order of E-6, E-7 for $m' = 96$, and on the order of E-6, E-7 for $m' = 192$. The exact solution and HWM solution for $\alpha = 1$ and $m' = 24$ is plotted in Figure 4 to illustrate the accuracy of the method. The FDE solutions for a few fractional values of α are presented in Figure 5. As can be seen from Figure 5, as the fractional α approaches 1, the approximate solution obtained for α approximates to the exact solution.

Table 4. The absolute errors for HWM for several m' of example 3.

t	$m' = 12$	$m' = 24$	$m' = 48$	$m' = 96$	$m' = 192$
0	1.00×10^{-3}	4.47×10^{-4}	1.54×10^{-4}	4.54×10^{-5}	1.24×10^{-5}
0.1	1.90×10^{-3}	3.63×10^{-4}	9.31×10^{-5}	2.49×10^{-5}	6.20×10^{-6}
0.2	6.26×10^{-4}	1.73×10^{-4}	4.97×10^{-5}	1.24×10^{-5}	3.00×10^{-6}
0.3	4.34×10^{-4}	1.08×10^{-4}	2.34×10^{-5}	5.90×10^{-6}	1.53×10^{-6}
0.4	1.24×10^{-4}	4.97×10^{-5}	1.23×10^{-5}	2.81×10^{-6}	7.05×10^{-7}
0.5	1.04×10^{-4}	7.99×10^{-6}	8.56×10^{-7}	6.21×10^{-7}	2.10×10^{-7}
0.6	2.26×10^{-5}	2.09×10^{-6}	3.80×10^{-7}	2.84×10^{-8}	5.79×10^{-9}
0.7	5.47×10^{-5}	1.25×10^{-5}	2.42×10^{-6}	6.12×10^{-7}	1.64×10^{-7}
0.8	6.02×10^{-5}	1.51×10^{-5}	4.29×10^{-6}	1.06×10^{-6}	2.58×10^{-7}
0.9	9.23×10^{-5}	1.98×10^{-5}	4.98×10^{-6}	1.29×10^{-6}	3.23×10^{-7}

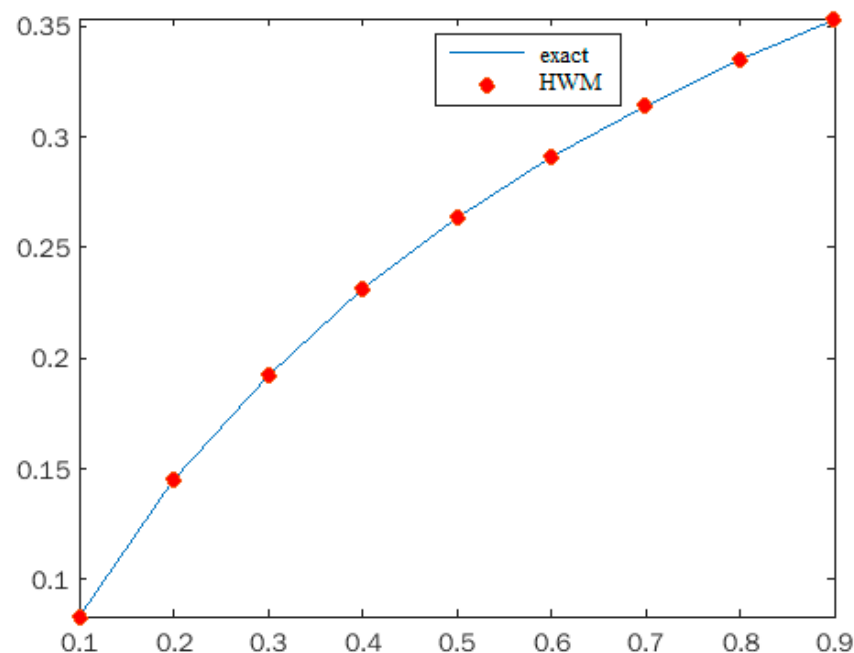


Figure 4. HWM result for $\alpha = 1$ with the exact solution of example 3 for $m' = 24$.

Example 4:

Consider the FDE [34] given below for $0 < \alpha \leq 1$ and $0 \leq t < 1$:

$$D^\alpha y(t) + y^2(t) - 1 = 0 \text{ with } y(0) = 0. \quad (44)$$

The exact solution for $\alpha = 1$ is given as $y(t) = \frac{e^{2t} - 1}{e^{2t} + 1}$.

The application of HW method to the FDE yields:

$$C^T \phi_{m'xm'} + [a_1^2, a_2^2, \dots, a_{m'}^2] - [1, 1, \dots, 1] = 0 \tag{45}$$

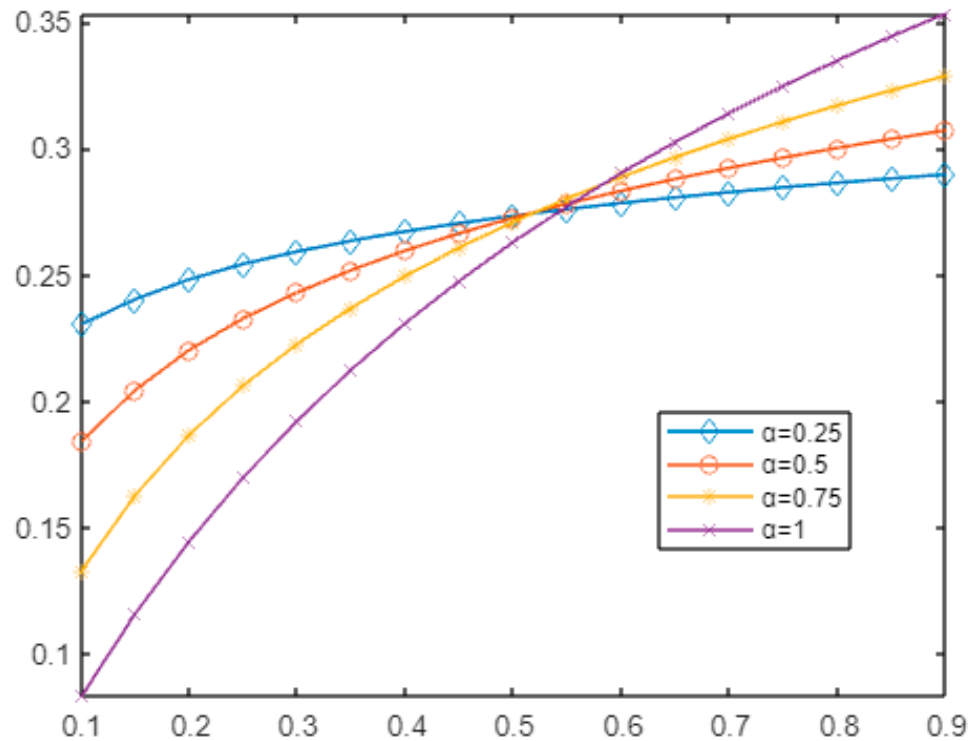


Figure 5. HWM result for several values of α of example 3 for $m' = 24$.

The solution for (45) is obtained as with the previous example through the algebraic system of equations, constructed using a few collocation points. This example was chosen to provide comparison with several other numerical methods presented elsewhere. Table 5 gives the results for several m' values of the proposed method, and also includes the results of Modified Homotopy Perturbation Method (MHPM) [34] and Iterative Reproducing Kernel Hilbert Spaces Method (IRKHSM) [35] for $\alpha = 1$. The results show that HWM produces smaller errors for the most t values even when $m' = 48$, for $m' \geq 96$ HWM is a better approximation method. Table 6 summarizes the comparative results for fractional $\alpha = 0.75$ of the proposed method and also of the Reproducing Kernel Method (RKM) [36], Bernstein Polynomial Method (BPM) [37], Iterative Reproducing Kernel Hilbert Spaces Method (IRKHSM) [38], Haar Wavelet Operational Matrix Method (HWOMM) [39] and Modified Homotopy Perturbation Method (MHPM) [34]. For the fractional α there is not an exact solution, all results are relatively close to one another. Therefore, the results of the proposed method can be interpreted as producing an acceptable outcome for the fractional α .

Table 5. Absolute errors for HWM for several m' and comparison with the Modified Homotopy Perturbation Method (MHPM) [34] and Iterative Reproducing Kernel Hilbert Spaces Method (IRKHSM) [35] for $\alpha = 1$.

t	$m' = 12$	$m' = 24$	$m' = 48$	$m' = 96$	$m' = 192$	$m' = 384$	MHPM [34]	IRKHSM [35]
0.1	6.40×10^{-5}	3.24×10^{-5}	7.88×10^{-6}	1.71×10^{-6}	4.31×10^{-7}	1.10×10^{-8}	0	9.05×10^{-6}
0.2	2.44×10^{-4}	5.91×10^{-5}	1.29×10^{-5}	3.25×10^{-6}	8.42×10^{-7}	1.12×10^{-7}	0	1.72×10^{-5}
0.3	2.71×10^{-4}	6.82×10^{-5}	1.85×10^{-5}	4.60×10^{-6}	1.13×10^{-6}	2.10×10^{-7}	1.00×10^{-6}	2.38×10^{-5}
0.4	3.64×10^{-4}	8.24×10^{-5}	2.06×10^{-5}	5.29×10^{-6}	1.32×10^{-6}	2.82×10^{-7}	5.00×10^{-6}	2.85×10^{-5}

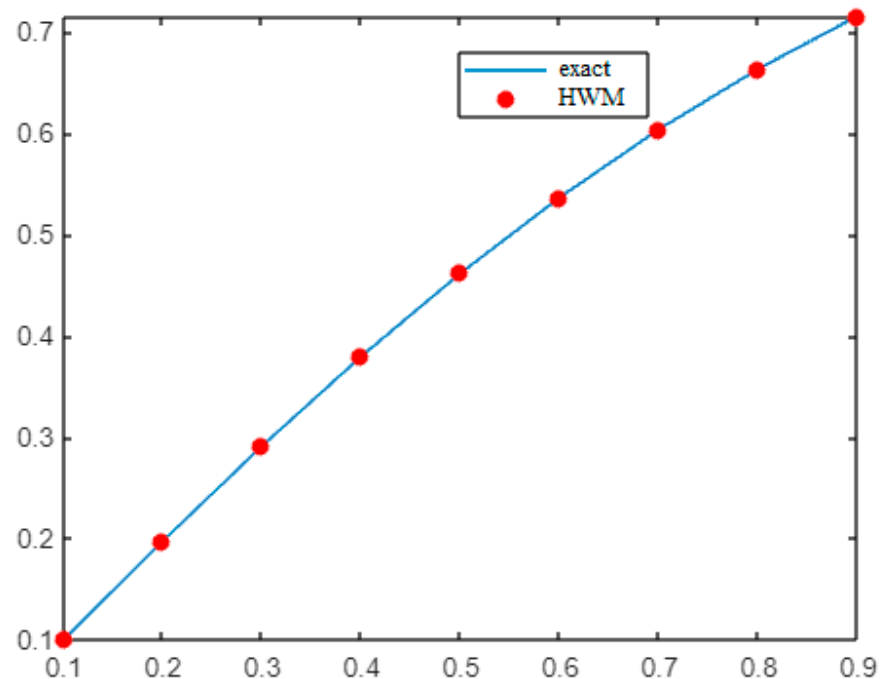
Table 5. Cont.

t	$m' = 12$	$m' = 24$	$m' = 48$	$m' = 96$	$m' = 192$	$m' = 384$	MHPM [34]	IRKHSM [35]
0.5	3.92×10^{-4}	9.67×10^{-5}	2.33×10^{-5}	5.68×10^{-6}	1.40×10^{-6}	3.28×10^{-7}	3.90×10^{-5}	3.11×10^{-5}
0.6	3.35×10^{-4}	8.53×10^{-5}	2.13×10^{-5}	5.29×10^{-6}	1.32×10^{-6}	3.46×10^{-7}	1.93×10^{-4}	3.17×10^{-5}
0.7	3.05×10^{-4}	7.56×10^{-5}	1.90×10^{-5}	4.75×10^{-6}	1.19×10^{-6}	3.31×10^{-7}	7.37×10^{-4}	3.07×10^{-5}
0.8	2.62×10^{-4}	6.47×10^{-5}	1.58×10^{-5}	3.95×10^{-6}	9.93×10^{-7}	2.96×10^{-7}	2.33×10^{-3}	2.81×10^{-5}
0.9	1.84×10^{-4}	5.03×10^{-5}	1.25×10^{-5}	3.06×10^{-6}	7.65×10^{-7}	2.48×10^{-7}	6.37×10^{-3}	2.32×10^{-5}

Table 6. Comparison with the Reproducing Kernel Method (RKM) [36], Bernstein Polynomial Method (BPM) [37], Iterative Reproducing Kernel Hilbert Spaces Method (IRKHSM) [38], Haar Wavelet Operational Matrix Method (HWOMM) [39], and Modified Homotopy Perturbation Method (MHPM) [34] for $\alpha = 0.75$.

t	$m' = 384$	RKM [36]	BPM [37]	IRKHSM [38]	HWOMM [39]	MHPM [34]
0.2	0.309974	0.3073	0.3099	0.3100	0.3095	0.3138
0.4	0.481631	0.4803	0.4816	0.4816	0.4814	0.4929
0.6	0.597783	0.5975	0.5977	0.5978	0.5977	0.5974
0.8	0.678849	0.6796	0.6788	0.6788	0.6788	0.6604

The exact and HWM results are plotted in Figure 6 for $\alpha = 1$. Figure 7 includes plots for several α . As with the other examples, the fractional approximate solutions approach the exact result obtained for $\alpha = 1$ as α approaches 1.

**Figure 6.** HWM result for $\alpha = 1$ with the exact solution of Example 4 for $m' = 24$.

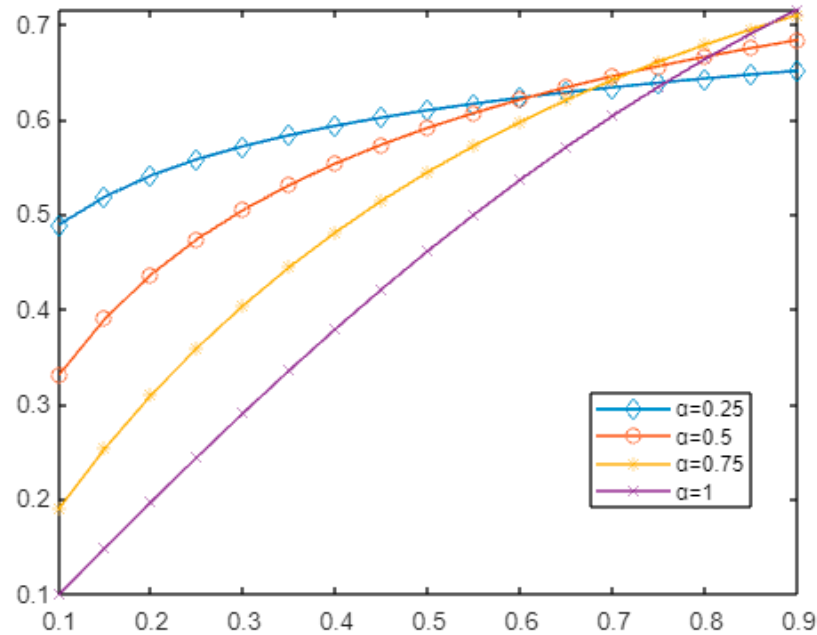


Figure 7. HWM result for several values of α of Example 4 for $m' = 24$.

8. Conclusions

The motivation for this study stems from the need to employ Hermite wavelets for the numeric solution of nonlinear FDEs. To the best of our knowledge, the HWs have not been explored much in this regard. The operational matrices required for each of the fractional terms in the FDE to convert it to an algebraic equation are sparser due to the orthogonality of the Hermite wavelets. The orthogonality property is essential for the lower computational load and fast convergence of the method. The HW method is very accurate, even for the small number of collocation points, as demonstrated in the numerical examples. The maximum errors are generally on the order of E-5–E-7 for the collocation points up to $m' = 96$. For higher accuracy, the number of the collocation points must be increased. Additionally, the resulting algebraic equation for numeric approximation is a vector-matrix equation. The compactness obtained in vector-matrix form facilitates the coding process of the method. The convergence analysis is also provided for the proposed method.

As can be seen from Figures 3, 5 and 7, the numerical solutions for the fractional values of α approach the solution obtained for $\alpha = 1$ as α approaches 1, which verifies the solutions obtained for fractional α values.

We believe the work presented here can be employed in a wide variety of applications such as variable-order models, systems of FDEs, systems of integro-fractional differential equations, optimal control problems, and fractional partial differential equations.

Author Contributions: Conceptualization A.T.D.; methodology, A.T.D.; software, P.S. and S.N.T.P.; writing—original draft preparation, A.T.D. and S.N.T.P.; writing—review and editing, A.T.D. and S.N.T.P.; All authors have read and agreed to the published version of the manuscript.

Funding: This work was supported by Yildiz Technical University Scientific Research Projects Coordination Unit under project number FYL-2021-4342.

Data Availability Statement: Not applicable.

Acknowledgments: The authors are grateful for the support from Yildiz Technical University Scientific Research Projects Coordination Unit under project number FYL-2021-4342.

Conflicts of Interest: The authors declare no conflict of interest.

References

1. Arikoğlu, A.; Özkol, İ. Solution of fractional differential equations by using differential transform method. *Chaos Solitons Fractals* **2007**, *34*, 1473–1481. [[CrossRef](#)]
2. Li, X. Numerical solution of fractional differential equations using cubic *B*-spline wavelet collocation method. *Commun. Nonlinear Sci. Numer. Simul.* **2012**, *17*, 3934–3946. [[CrossRef](#)]
3. Erturk, V.S.; Momani, S. Solving systems of fractional differential equations using differential transform method. *J. Comput. Appl. Math.* **2008**, *215*, 142–151. [[CrossRef](#)]
4. Momani, S.; Odibat, Z. Numerical comparison of methods for solving linear differential equations of fractional order. *Chaos Solitons Fractals* **2007**, *31*, 1248–1255. [[CrossRef](#)]
5. Babolian, E.; Vahidi, A.R.; Shoja, A. An efficient method for nonlinear fractional differential equations: Combination of the Adomian decomposition method and Spectral method. *Indian J. Pure Appl. Math.* **2014**, *45*, 1017–1028. [[CrossRef](#)]
6. Yang, S.; Xiao, A.; Su, H. Convergence of the variational iteration method for solving multi-order fractional differential equations. *Comput. Math. Appl.* **2010**, *60*, 2871–2879. [[CrossRef](#)]
7. Kumar, S.; Gupta, V. An application of variational iteration method for solving fuzzy time-fractional diffusion equations. *Neural. Comput. Appl.* **2021**, *33*, 17659–17668. [[CrossRef](#)]
8. Huang, J.; Tang, Y.; Vazquez, L. Convergence analysis of a block-by-block method for fractional differential equations. *Numer. Math. Theory Methods Appl.* **2012**, *5*, 229–241. [[CrossRef](#)]
9. Mokhtary, P.; Ghoreishi, F.; Srivastava, H.M. The Müntz-Legendre Tau method for fractional differential equations. *Appl. Math. Model.* **2016**, *40*, 671–684. [[CrossRef](#)]
10. Tural-Polat, S.N.; Dincel, A.T. Numerical solution method for multi-term variable order fractional differential equations by shifted chebyshev polynomials of the third kind. *Alex. Eng. J.* **2022**, *61*, 5145–5153. [[CrossRef](#)]
11. Azarnavid, B.; Emamjomeh, M.; Nabati, M. A shooting like method based on the shifted Chebyshev polynomials for solving nonlinear fractional multi-point boundary value problem. *Chaos Solitons Fractals* **2022**, *159*, in press. [[CrossRef](#)]
12. Fambri, F.; Dumbser, M. Spectral semi-implicit and space-time discontinuous Galerkin methods for the incompressible Navier-Stokes equations on staggered Cartesian grids. *Appl. Numer. Math.* **2016**, *110*, 41–74. [[CrossRef](#)]
13. Yüzbaşı, S. Numerical solution of the Bagley-Torvik equation by the Bessel collocation method. *Math. Method Appl. Sci.* **2013**, *36*, 300–312. [[CrossRef](#)]
14. Pindza, E.; Owolabi, K.M. Fourier spectral method for higher order space fractional reaction-diffusion equations. *Commun. Nonlinear Sci.* **2016**, *40*, 112–128. [[CrossRef](#)]
15. Al-Smadi, M.; Abu Arqub, O. Computational algorithm for solving fredholm time-fractional partial integro differential equations of dirichlet functions type with error estimates. *Appl. Math. Comput.* **2019**, *342*, 280–294.
16. Al-Smadi, M.; Abu Arqub, O.; Gaith, M. Numerical simulation of telegraph and Cattaneo fractional-type models using adaptive reproducing kernel framework. *Math. Methods Appl. Sci.* **2021**, *44*, 8472–8489. [[CrossRef](#)]
17. Bengochea, G. Operational solution of fractional differential equations. *Appl. Math. Lett.* **2014**, *32*, 48–52. [[CrossRef](#)]
18. Luchko, Y.; Gorenflo, R. An operational method for solving fractional differential equations with the Caputo derivatives. *Acta Math. Vietnam.* **1999**, *24*, 207–233.
19. Li, M.; Zhao, W. Solving Abel's type integral equation with Mikusinski's operator of fractional order. *Adv. Math. Phys.* **2013**, *2013*, 806984.
20. Xu, X.Y.; Xu, D. Legendre wavelets method for approximate solution of fractional-order differential equations under multi-point boundary conditions. *Int. J. Comput. Math.* **2018**, *95*, 998–1014. [[CrossRef](#)]
21. Rahimkhani, P.; Ordokhani, Y.; Babolian, E. An efficient approximate method for solving delay fractional optimal control problems. *Nonlinear Dynam.* **2016**, *86*, 1649–1661. [[CrossRef](#)]
22. Rehman, M.U.; Khan, R.A. A numerical method for solving boundary value problems for fractional differential equations. *Appl. Math. Model.* **2012**, *36*, 894–907. [[CrossRef](#)]
23. Shiralashetti, S.C.; Hanaji, S.I. Taylor wavelet collocation method for Benjamin–Bona–Mahony partial differential equations. *Results Appl. Math.* **2021**, *9*, 100139. [[CrossRef](#)]
24. Shiralashetti, S.C.; Kumbinarasaiah, S. CAS wavelets analytic solution and Genocchi polynomials numerical solutions for the integral and integro-differential equations. *J. Interdiscip. Math.* **2019**, *22*, 201–218. [[CrossRef](#)]
25. Kumbinarasaiah, S.; Mundewadi, R.A. Numerical solution of fractional-order integro-differential equations using Laguerre wavelet method. *J. Optim. Theory Appl.* **2022**, in press. [[CrossRef](#)]
26. Behera, S.; Saha Ray, S. Euler wavelets method for solving fractional-order linear Volterra–Fredholm integro-differential equations with weakly singular kernels. *Comp. Appl. Math.* **2021**, *40*, 1–30. [[CrossRef](#)]
27. Zhu, L.; Wang, Y. Second Chebyshev wavelet operational matrix of integration and its application in the calculus of variations. *Int. J. Comput. Math.* **2013**, *90*, 2338–2352. [[CrossRef](#)]
28. Lal, S.; Sharma, R.P. Approximation of function belonging to generalized Hölder's class by first and second kind Chebyshev wavelets and their applications in the solutions of Abel's integral equations. *Arab. J. Math.* **2021**, *10*, 157–174. [[CrossRef](#)]
29. Shiralashetti, S.C.; Kumbinarasaiah, S. Hermite wavelets operational matrix of integration for the numerical solution of nonlinear singular initial value problems. *Alex. Eng. J.* **2018**, *57*, 2591–2600. [[CrossRef](#)]

30. Podlubny, I. *Fractional Differential Equations: An Introduction to Fractional Derivatives, Fractional Differential Equations, to Methods of Their Solution and Some of Their Applications*; Academic Press: Cambridge, MA, USA, 1998.
31. Kilicman, A.; Al Zhour, Z.A.A. Kronecker operational matrices for fractional calculus and some applications. *Appl. Math. Comput.* **2007**, *187*, 250–265. [[CrossRef](#)]
32. Li, Y.; Sun, N. Numerical solution of fractional differential equations using the generalized block pulse operational matrix. *Comput. Math. Appl.* **2011**, *62*, 1046–1054. [[CrossRef](#)]
33. Saad, K.M.; Al-Shomrani, A.A. An application of homotopy analysis transform method for Riccati differential equation of fractional order. *J. Fract. Calc. Appl.* **2016**, *7*, 61–72.
34. Odibat, Z.; Momani, S. Modified homotopy perturbation method: Application to quadratic Riccati differential equation of fractional order. *Chaos Solitons Fractals* **2008**, *36*, 167–174. [[CrossRef](#)]
35. Sakar, M. Iterative reproducing kernel Hilbert spaces method for Riccati differential equations. *J. Comput. Appl. Math.* **2017**, *309*, 163–174. [[CrossRef](#)]
36. Li, X.Y.; Wu, B.Y.; Wang, R.T. Reproducing kernel method for fractional Riccati differential equations. *Abstr. Appl.* **2014**, *2014*, 970967. [[CrossRef](#)]
37. Yüzbaşı, S. Numerical solutions of fractional Riccati type differential equations by means of the Bernstein polynomials. *Appl. Math. Comput.* **2013**, *219*, 6328–6343. [[CrossRef](#)]
38. Sakar, M.G.; Akgül, A.; Baleanu, D. On solutions of fractional Riccati differential equations. *Adv. Differ. Equ.* **2017**, *39*, 1–10. [[CrossRef](#)]
39. Li, Y.; Sun, N.; Zheng, B.; Wang, Q.; Zhang, Y. Wavelet operational matrix method for solving the Riccati differential equation. *Commun. Nonlinear Sci. Numer. Simul.* **2014**, *19*, 483–493. [[CrossRef](#)]

Disclaimer/Publisher's Note: The statements, opinions and data contained in all publications are solely those of the individual author(s) and contributor(s) and not of MDPI and/or the editor(s). MDPI and/or the editor(s) disclaim responsibility for any injury to people or property resulting from any ideas, methods, instructions or products referred to in the content.